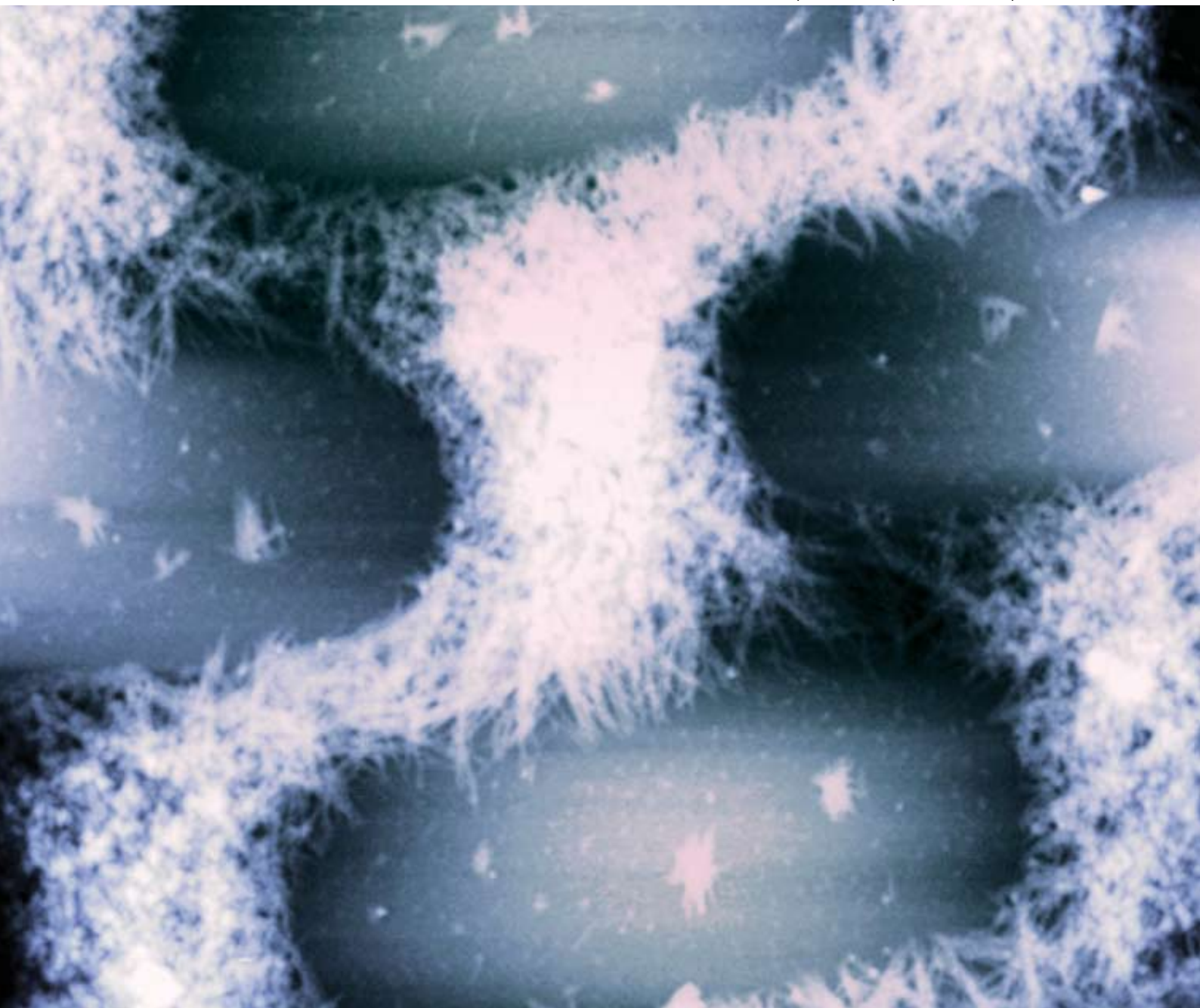


Soft Matter

www.softmatter.org

Volume 5 | Number 8 | 21 April 2009 | Pages 1541–1744



ISSN 1744-683X

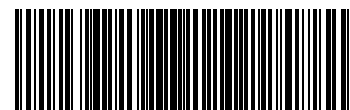
RSC Publishing

COMMUNICATION

Zhiqun Lin *et al.*
Controlled evaporative self-assembly of hierarchically structured regioregular conjugated polymers

HIGHLIGHT

Aiwu Sun and Joerg Lahann
Dynamically switchable biointerfaces



1744-683X(2009)5:8;1-E

Controlled evaporative self-assembly of hierarchically structured regioregular conjugated polymers†

Myunghwan Byun,^a Robyn L. Laskowski,^b Ming He,^c Feng Qiu,^c Malika Jeffries-EL^b and Zhiqun Lin^{*a}

Received 24th December 2008, Accepted 23rd January 2009

First published as an Advance Article on the web 18th February 2009

DOI: 10.1039/b822998h

A toluene solution of the semiconducting conjugated polymer regioregular poly(3-hexylthiophene) (*rr*-P3HT) was confined in a sphere-on-flat geometry, forming an axially symmetric, capillary-held microfluid, from which the consecutive “stick–slip” motion of the contact line of the solution *via* solvent evaporation was effectively regulated. As a result, hierarchical “snake-skin” like structures of high regularity were obtained where each microscopic ellipsoid within the “snake-skin” was composed of bundles of *rr*-P3HT nanofibers. This facile, *one-step* deposition technique based on controlled evaporative self-assembly opens up a new avenue for organizing semicrystalline conjugated polymers into two-dimensional ordered patterns in a simple, cost-effective, and controllable manner.

Introduction

Of the various conjugated polymers, regioregular poly(3-hexylthiophene) (*rr*-P3HT) is among the most widely studied conjugated polymers. It has a rather rigid backbone with a regular head-to-tail arrangement of pendant hexyl side chains that allow for efficient π – π stacking of the conjugated backbones and solubilization.^{1–8} *rr*-P3HT chains self-organize to form nanoscopic crystalline structures, which are dramatically influenced by regioregularity,⁹ molecular weight,^{10–14} solvent properties,^{11,15} and processing conditions (spin-coating, dip coating and drop casting),¹⁵ resulting in variations of the charge carrier mobility in thin-film transistors by several orders of magnitude.¹⁵ *rr*-P3HT possesses high solubility in a variety of organic solvents and excellent film-forming properties, making it an attractive material for use as a printable semiconducting polymer.⁷ Successful implementation of *rr*-P3HT for use in low-cost microelectronic and optoelectronic applications, for example, organic thin-film transistors, requires simple strategies to deposit and arrange *rr*-P3HT into well-ordered patterns over large areas with controlled coverage.^{16–20}

Evaporative self-assembly of nonvolatile solutes (*e.g.*, polymers and colloidal particles) from a sessile drop is an emergent surface-patterning technique for potential application in optical,

microelectronics, and sensory devices. However, the dissipative structures created *via* evaporation, including polygonal network structures,^{21–24} fingering instabilities,^{25,26} and familiar multiple “coffee rings”,^{27–29} are often irregular and without controllable spacing and size. Thus, a challenge that remains is to control the evaporation process (*e.g.*, evaporation flux, solution concentration, and interfacial interaction between the solute and the substrate), so intriguing and highly ordered structures on a large scale can be produced rapidly and economically.

Here, we present the surface-patterning of a luminescent conjugated polymer, *rr*-P3HT, into highly ordered, hierarchically structured microscopic “snake-skin” like patterns. This is a direct consequence of controlled evaporative self-assembly of *rr*-P3HT in a confined geometry composed of a spherical lens on a flat substrate (*i.e.*, sphere-on-flat geometry; Fig. 1a and 1b) in conjunction with strong intermolecular interaction of P3HT chains (*i.e.*, interchain π – π stacking). This facile, *one-step* deposition technique based on controlled evaporative self-assembly opens up a new avenue for organizing semicrystalline conjugated polymers into two-dimensional ordered patterns in a simple, cost-effective, and controllable manner for potential applications in optoelectronics, photonics, and biosensors, among other areas.

Results and discussion

The choice of *rr*-P3HT as the nonvolatile solute was motivated by its promising applications in thin-film transistors (high field-effect

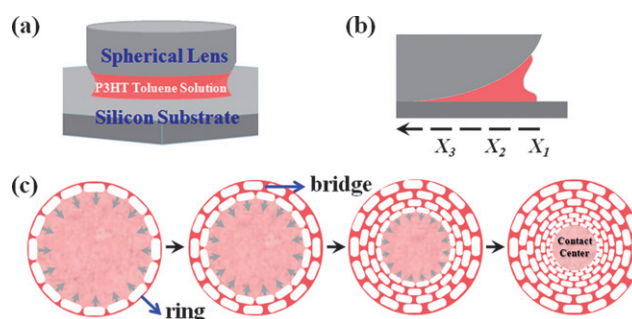


Fig. 1 (a) Schematic illustration of the sphere-on-flat geometry in which a drop of P3HT toluene solution was constrained, forming a capillary-held solution between the spherical lens and the Si substrate. (b) Close-up, cross-sectional view of the right capillary edge, where X_n ($n = 1–3$) indicates the radial position away from the sphere/Si contact center. (c) Stepwise representation of the formation of two-dimensional “snake-skin” like structures from the 0.1 mg/mL P3HT toluene solution. The sphere/Si contact area is marked as the “Contact Center” in the far right panel.

^aDepartment of Materials Science and Engineering, Iowa State University, Ames, IA, 50011. E-mail: zqlin@iastate.edu; Tel: +515-294-9967

^bDepartment of Chemistry, Iowa State University, Ames, IA, 50011

^cDepartment of Macromolecular Science and the Key Laboratory of Molecular Engineering of Polymers at Fudan University, Shanghai, China 200433

† Electronic supplementary information (ESI) available: Optical micrographs and AFM images of dotted arrays and a continuous film obtained from the 0.01 mg/mL and 0.5 mg/mL P3HT toluene solutions. See DOI: 10.1039/b822998h

mobility, $0.1 \text{ cm}^2 \text{ V}^{-1} \text{ s}^{-1}$)^{11–15} and solar cells.^{30–33} The 0.1 mg/ml P3HT toluene solution was loaded and trapped in between the sphere and the Si substrate, yielding a capillary-held solution (Fig. 1a and b) from which toluene was allowed to evaporate only at the capillary edge (Fig. 1b). As the toluene evaporated, P3HT was transported from the solution inside to the capillary edge and pinned at the contact line (*i.e.*, “stick”), forming a “coffee ring” (far left panel in Fig. 1c). During the deposition of P3HT, the initial contact angle gradually decreased to a critical contact angle, at which the capillary force (*i.e.*, depinning force) becomes larger than the pinning force,³⁴ leading the contact line to jerk (*i.e.*, “slip”) to the next position inward, where it was pinned again and a new ring was thus yielded (second panel from the left in Fig. 1c). It is noteworthy that two adjacent rings were connected by periodically arranged P3HT “bridges” that originated from fingering instabilities emerging at the ring (Fig. 1c). The use of rationally designed, axially symmetric sphere-on-Si geometry rendered control over the solvent evaporation, resulting in a controlled, repetitive “stick–slip” motion of the contact line of the P3HT toluene solution, and ultimately yielding a “snake-skin” like network over a large area (far right panel in Fig. 1c).

A representative fluorescence micrograph of highly ordered P3HT “snake-skin” is shown in Fig. 2a. The “snake-skin” possessed gradient features in terms of the distances between adjacent rings, λ_C , and between adjacent bridges, λ_F , (Fig. 2a and Fig. 3) as the solution front (*i.e.*, liquid capillary edge) approached the sphere/Si contact center. This is because of the imbalance of the nonlinear capillary force (*i.e.*, depinning force) due to the curvature effect of the sphere, and linear pinning force.³⁴ Locally, they appear as elongated honeycombs as revealed by the AFM measurement (Fig. 2b). λ_C and λ_F progressively decreased from $\lambda_C = 14.3 \mu\text{m}$ and $\lambda_F = 10.7 \mu\text{m}$ at the outermost region, $X_1 = 3720 \mu\text{m}$, to $\lambda_C = 12.5 \mu\text{m}$ and $\lambda_F = 8.4 \mu\text{m}$ at the intermediate region, $X_2 = 2860 \mu\text{m}$, to $\lambda_C = 9.8 \mu\text{m}$ and $\lambda_F = 6.6 \mu\text{m}$ at the innermost region, $X_3 = 2150 \mu\text{m}$ (Fig. 3b), where X_n corresponds to the distance from the sphere/Si contact center as illustrated in Fig. 1b and Fig. 3a.

Close examination of the P3HT “snake-skins” by AFM revealed that each ellipsoid (*i.e.*, elongated honeycomb) within the “snake-skin” was composed of bundles of nanoscopic P3HT fibers (Fig. 4). Since P3HT is a regioregular semicrystalline molecule, a P3HT nanofiber was formed by strong interchain π – π stacking of

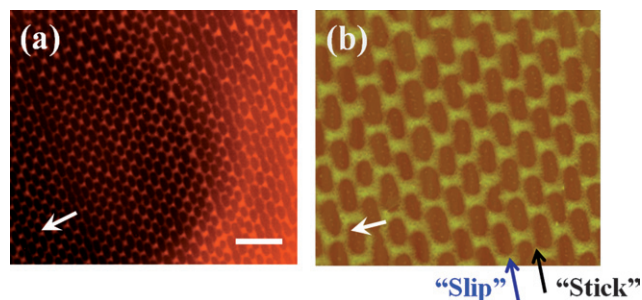


Fig. 2 (a) Representative fluorescence micrograph of 2D P3HT interconnected structures obtained from drying-mediated self-assembly of the 0.1 mg/mL P3HT toluene solution, resembling the “snake-skin” morphology. Scale bar = $35 \mu\text{m}$. (b) The corresponding AFM height image of “snake-skin” like structures. Scan size = $70 \times 70 \mu\text{m}^2$. Arrows indicate the moving direction of the solution front during the course of evaporation.

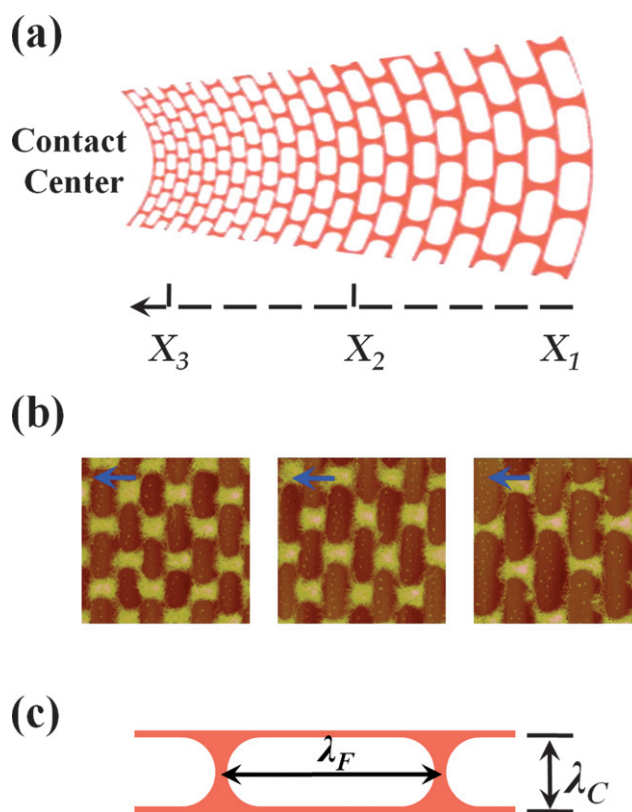


Fig. 3 (a) Schematic illustration of a small zone of “snake-skin” like structures formed away from the sphere/Si contact center. The “snake-skin” possesses a gradient in terms of the distances between adjacent rings, λ_C , and between adjacent bridges, λ_F (c). (b) Representative AFM height images at the outermost region ($X_1 = 3200 \mu\text{m}$), the intermediate region ($X_2 = 2900 \mu\text{m}$), and the innermost region ($X_3 = 2600 \mu\text{m}$), respectively. Arrows mark the moving direction of the solution front during the course of evaporation. Scan size = $30 \times 30 \mu\text{m}^2$ in all images. (c) Schematic showing the dimensions of λ_C and λ_F .

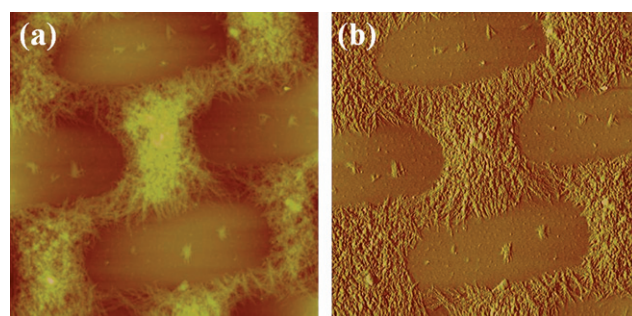


Fig. 4 Typical AFM height (a) and phase (b) images, showing that the mesoscale P3HT “snake-skin” is composed of P3HT nanofibers. Scan size = $15 \times 15 \mu\text{m}^2$.

crystalline lamellae with the P3HT chains oriented perpendicular to the long axis of the nanofiber (*i.e.* the π – π stacking direction).^{7,11,35} The nanofibrillar morphologies are widely observed in low molecular weight P3HT films prepared by considerably slow deposition techniques and/or using solvents with a high boiling point,^{7,15,35} while the fast solvent evaporation suppressed the self-assembly of P3HT nanofibrils.³⁶ In the present study, the MW of P3HT was low

(MW = 13.5K) and the evaporation rate of toluene was slow due to the use of the sphere-on-Si geometry where the solution was allowed to evaporate only at the capillary edge: it took approximately 30 min for evaporation to be complete, thereby facilitating the formation of P3HT nanofibers. As a result, the P3HT “snake-skins” were hierarchically structured, composed of gradient microscopic ellipsoids in which numerous nanofibers were randomly overlapped, especially in the “bridges”.

Based on the *in situ* optical microscopy observation in reflection mode, the formation of intriguing, hierarchically structured P3HT patterns may be rationalized as follows. As the toluene evaporated, the contact line of the P3HT toluene solution was arrested for a certain period of time (*i.e.*, forming P3HT “coffee rings”), during which the fingering instabilities emerged normal to the ring (far left panel in Fig. 1c); they served as nucleation sites. The P3HT chains do not entangle one another due to their rigid rod-like nature as compared to the random coil-like polymers. Moreover, the MW of the P3HT was low. Taken together, P3HT fingers may be easily formed (Fig. 1c). Subsequently, the solution front jerked to the next position, during which the fingers grew into “bridges”, consisting of P3HT nanofiber bundles, by primarily transporting P3HT nanofibers from the solution inside to the capillary edge. It is plausible that a small portion of P3HT chains may also migrate (be pulled) along the previously formed ring to the “bridges”. At this new position, the contact line was pinned again, forming a new ring; the “bridges” and the rings were locked in upon complete evaporation of residual solvent. This process was repeated until the solution front was in close proximity to the sphere/Si contact center, thereby yielding massive P3HT “snake-skin” like network structures that were composed of regularly arranged “stick” motion-induced rings that were parallel to the contact line and radially oriented “bridges” that were perpendicular to the contact line.

It is worth noting that the solution concentration played an important role in the P3HT structure formation. In marked contrast with the “snake-skin” structures observed exclusively at $c = 0.1$ mg/ml, at lower concentration, $c = 0.01$ mg/ml, regularly arranged micrometre-sized P3HT dotted arrays were formed. A schematic representation of the formation of dotted arrays is depicted in Fig. S1, ESI†. The optical micrograph in reflection mode taken at the boundary of the outermost and the intermediate regions ($X_1 \approx X_2$) revealed that each individual ring was broken into dots due to the presence of residual solvent (*i.e.*, forming dotted lines; Fig. S2a, ESI†), indicating a surface tension driven Rayleigh instability at the pinned contact line that minimized the surface free energy and maximized the intermolecular π - π stacking of P3HT since the concentration was ten times more dilute in comparison to the 0.1 mg/ml solution. This observation resembled a recent study in drying-mediated self-assembly of a capillary-held organometallic poly(ferrocenyldimethylsilane) solution, where dotted poly(ferrocenyldimethylsilane) lines were produced at low concentration.³⁷ The characteristic distance between neighboring P3HT microdots from adjacent dotted lines, λ_c was 5.6 μm at the boundary of the outermost and the intermediate regions ($X_1 \approx X_2$) = 3300 μm , and 4.2 μm at the boundary of the intermediate and the inner regions, ($X_2 \approx X_3$) = 2500 μm (Fig. S2b, ESI†). Each individual dot was composed of aggregated P3HT nanofibers (Fig. S3, ESI†). On the other hand, it is not surprising that when a higher concentration P3HT toluene solution was used ($c = 0.5$ mg/ml), a continuous P3HT film was deposited on the Si substrate (Fig. S4, ESI†).

Materials and methods

Synthesis of regioregular conjugated *rr*-P3HT

rr-P3HT was synthesized *via* a quasi-living polymerization.^{1,38} The synthesis details are described as follows. In a three neck round bottom flask, 2,5-dibromo-3-hexylthiophene (1.63g, 5.0 mmol) was dissolved in THF (10 mL) and stirred under N_2 . *tert*-Butylmagnesium chloride (2.5 mL, 5.0 mmol) was added *via* syringe and the mixture was stirred at room temperature for 2 h. The reaction mixture was then diluted to 50 mL with THF and Ni(dppp)Cl₂ (45 mg, 0.082 mmol) was added in one portion. The mixture was stirred for 10 mins at room temperature, and then poured into methanol to precipitate the P3HT. The polymer was filtered into an extraction thimble and washed by Soxhlet extraction with methanol, hexanes, and chloroform. Finally, P3HT was recovered from the chloroform solution by evaporation. The regioregularity of P3HT was greater than 98% as determined by ¹H NMR.¹² The number average molecular weight and polydispersity index of P3HT were 13 500 g/mol and 1.12, respectively, as measured by GPC.

Evaporative self-assembly of hierarchically structured P3HT in a sphere-on-flat geometry

The above mentioned *rr*-P3HT was selected as the nonvolatile solute to prepare P3HT toluene solutions at the concentration $c = 0.1$ mg/ml. Si wafer and the spherical lens, made from fused silica (radius of curvature, $R = 1.65$ cm, and diameter, $D = 1$ cm), were cleaned with a mixture of sulfuric acid and Nonchromix. After sonication for 30 min, they were extensively rinsed with DI water and blown dry with N_2 . A sphere-on-flat geometry (*i.e.*, sphere-on-Si) was constructed and implemented as follows.^{37,39–48} First, both the spherical lens and Si substrate were firmly fixed at the top and bottom of sample holders, respectively. Next, an inchworm motor was applied to bring the upper sphere into near contact with the lower stationary Si substrate. With just a few hundred micrometres between the surfaces, 18 μL of P3HT toluene solution was loaded and trapped between the sphere and Si due to capillary forces. Finally, the sphere was brought into contact with Si. As a result, a capillary-held P3HT toluene solution was formed with the evaporation rate highest at the edge of the capillary, as schematically illustrated in Fig. 1a and b. This geometry led to a controlled, repetitive “stick-slip” motion of the three-phase contact line, which moved towards the sphere/Si contact center (Fig. 1a–b) during the course of toluene evaporation. The sphere/Si contact area was marked as the “Contact Center” in the far right panel of Fig. 1c. The experiments were conducted in a sealed chamber in order to eliminate possible air convection, temperature gradient, and humidity effects. As a result, two-dimensional *rr*-P3HT “snake-skin” like patterns were formed on the surfaces of the spherical lens and the Si substrate. The complete evaporation took approximately 30 min. Only the patterns formed on the Si substrate were further examined in the study due to the curvature effect of the upper spherical surface.

Characterization

An Olympus BX51 optical microscope in the reflection, dark field, or fluorescence mode was used to monitor the morphological evolution of P3HT patterns in real time and examine the surface morphology after the sphere and Si surfaces were separated. AFM images on

patterns formed on a Si surface were performed using a Dimension 3100 scanning force microscope in tapping mode (Digital Instruments). BS-tap300 tips (Budget Sensors) with spring constants ranging from 20 to 75 Nm^{-1} were used as scanning probes.

Conclusions

In summary, by subjecting the P3HT toluene solution to evaporation in an axially symmetric sphere-on-flat geometry, hierarchically structured microscopic “snake-skin” like patterns were yielded *via* the synergy of controlled evaporative self-assembly of regioregular P3HT at the microscopic scale (*i.e.*, forming ellipsoids) and the strong intermolecular interaction of P3HT chains at the nanoscale (*i.e.*, responsible for the formation of bundles of P3HT nanofibers within the ellipsoid). By extension, it should be possible to form such highly ordered luminescent structures with other semi-crystalline conjugated polymers. This controlled evaporative self-assembly technique is fast, cost-effective, and robust, dispensing with the need for lithography and external fields. As such, it represents a powerful strategy for creating highly structured, multifunctional materials and devices for potential applications in optoelectronics, photonics, and biosensors, among other areas.

Acknowledgements

We gratefully acknowledge support from the National Science Foundation (NSF CAREER Award, CBET-0844084) and the Key Laboratory of Molecular Engineering of Polymers at Fudan University (Ministry of Education, China). We also thank Jianfeng Xia for discussion and Qingze Zou for AFM usage.

Notes and references

- 1 M. Jeffries-El, G. Sauve and R. D. McCullough, *Macromolecules*, 2005, **38**, 10346.
- 2 M. Jeffries-El, G. Sauve and R. D. McCullough, *Adv. Mater.*, 2004, **16**, 107.
- 3 M. C. Iovu, M. Jeffries-El, E. E. Sheina, J. R. Cooper and R. D. McCullough, *Polymer*, 2005, **46**, 8582.
- 4 M. C. Iovu, E. E. Sheina, R. R. Gil and R. D. McCullough, *Macromolecules*, 2005, **38**, 8649.
- 5 E. E. Sheina, J. Liu, M. C. Iovu, D. W. Laird and R. D. McCullough, *Macromolecules*, 2004, **37**, 3526.
- 6 K. M. Coakley, Y. X. Liu, M. D. McGehee, K. L. Findell and G. D. Stucky, *Adv. Funct. Mater.*, 2003, **13**, 301.
- 7 H. Yang, T. J. Shin, L. Yang, K. Cho, C. Y. Ryu and Z. Bao, *Adv. Funct. Mater.*, 2005, **15**, 671.
- 8 A. Babel, Y. Zhu, K. F. Cheng, W. C. Chen and S. A. Jenekhe, *Adv. Funct. Mater.*, 2007, **17**, 2542.
- 9 H. Sirringhaus, P. J. Brown, R. H. Friend, M. M. Nielsen, K. Bechgaard, B. M. W. Langeveld-Voss, A. J. H. Spiering, R. A. J. Janssen, E. W. Meijer, P. Herwig and D. M. de Leeuw, *Nature*, 1999, **401**, 685.
- 10 R. J. Kline, M. D. McGehee, E. N. Kadnikova, J. Liu and J. M. J. Frechet, *Adv. Mater.*, 2003, **15**, 1519.
- 11 R. J. Kline, M. D. McGehee, E. N. Kadnikova, J. Liu, J. M. J. Frechet and M. F. Toney, *Macromolecules*, 2005, **38**, 3312.
- 12 R. J. Kline, M. D. McGehee and M. F. Toney, *Nature Mater.*, 2006, **5**, 222.
- 13 R. Zhang, B. Li, M. C. Iovu, M. Jeffries-El, G. Sauve, J. Cooper, S. Jia, S. Tristram-Nagle, D. M. Smilgies, D. N. Lambeth, R. D. McCullough and T. Kowalewski, *J. Am. Chem. Soc.*, 2006, **128**, 3480.
- 14 A. Zen, J. Pflaum, S. Hirschmann, W. Zhuang, F. Jaiser, U. Asawapirom, J. P. Rabe, U. Scherf and D. Neher, *Adv. Funct. Mater.*, 2004, **14**, 757.
- 15 J.-F. Chang, B. Sun, D. W. Breiby, M. M. Nielson, T. I. Solling, M. Giles, I. McCulloch and H. Sirringhaus, *Chem. Mater.*, 2004, **16**, 4772.
- 16 Z. Bao, Y. Feng, A. Dodabalapur, V. R. Raju and A. J. Lovinger, *Chem. Mater.*, 1997, **9**, 1299.
- 17 J. A. Rogers, Z. Bao, A. Makhija and P. Braun, *Adv. Mater.*, 1999, **11**, 741.
- 18 S. Holdcroft, *Adv. Mater.*, 2001, **13**, 1753.
- 19 G. Derue, S. Coppee, S. Gabriele, M. Surin, V. Geskin, F. Monteverde, P. Leclere, R. Lazzaroni and P. Damman, *J. Am. Chem. Soc.*, 2005, **127**, 8018.
- 20 C. Balocco, L. A. Majewski and A. M. Song, *Organic Electronics*, 2006, **7**, 500.
- 21 E. Rabani, D. R. Reichman, P. L. Geissler and L. E. Brus, *Nature*, 2003, **426**, 271.
- 22 M. O. Blunt, C. P. Martin, M. Ahola-Tuomi, E. Pauliac-Vaujour, P. Sharp, P. Nativo, M. Brust and P. J. Moriarty, *Nature Nanotech.*, 2007, **2**, 167.
- 23 C. P. Martin, M. O. Blunt, E. Pauliac-Vaujour, A. Stannard and P. Moriarty, *Phys. Rev. Lett.*, 2007, **99**, 116103.
- 24 P. Moriarty, M. D. R. Taylor and M. Brust, *Phys. Rev. Lett.*, 2002, **89**, 248303.
- 25 J. Huang, F. Kim, A. R. Tao, S. Connor and P. D. Yang, *Nature Mater.*, 2005, **4**, 896.
- 26 A. V. Lyushnin, A. A. Golovin and L. M. Pismen, *Phys. Rev. E*, 2002, **65**, 021602.
- 27 R. D. Deegan, O. Bakajin, T. F. Dupont, G. Huber, S. R. Nagel and T. A. Witten, *Nature*, 1997, **389**, 827.
- 28 E. Adachi, A. S. Dimitrov and K. Nagayama, *Langmuir*, 1995, **11**, 1057.
- 29 B. P. Khanal and E. R. Zubarev, *Angew. Chem. Int. Ed.*, 2007, **46**, 2195.
- 30 W. U. Huynh, J. J. Dittmer and A. P. Alivisatos, *Science*, 2002, **295**, 2425.
- 31 J. Xu, J. Wang, M. Mitchell, P. Mukherjee, M. Jeffries-El, J. W. Petrich and Z. Q. Lin, *J. Am. Chem. Soc.*, 2007, **129**, 12828.
- 32 Z. Q. Lin, *Chem. Eur. J.*, 2008, **14**, 6294.
- 33 M. D. Goodman, J. Xu, J. Wang and Z. Q. Lin, *Chem. Mater.*, 2009, **21**, in press.
- 34 J. Xu, J. Xia, S. W. Hong, Z. Q. Lin, F. Qiu and Y. L. Yang, *Phys. Rev. Lett.*, 2006, **96**, 066104.
- 35 J. Verilhac, G. LeBlvennec, D. Djurado, F. Rieutord, M. Chouiki, J. Travers and A. Pron, *Synthetic Metals*, 2006, **156**, 815.
- 36 J. S. Liu, E. Sheina, T. Kowaleski and R. D. McCullough, *Angew. Chem. Int. Ed.*, 2002, **41**, 329.
- 37 S. W. Hong, J. Xu, J. Xia, Z. Q. Lin, F. Qiu and Y. L. Yang, *Chem. Mater.*, 2005, **17**, 6223.
- 38 J. Liu and R. D. McCullough, *Macromolecules*, 2002, **35**, 9882–9889.
- 39 S. W. Hong, S. Giri, V. S. Y. Lin and Z. Q. Lin, *Chem. Mater.*, 2006, **18**, 5164.
- 40 S. W. Hong, J. Xu and Z. Q. Lin, *Nano Lett.*, 2006, **6**, 2949.
- 41 S. W. Hong, W. Jeong, H. Ko, M. R. Kessler, V. Tsukruk and Z. Q. Lin, *Adv. Funct. Mater.*, 2008, **18**, 2114.
- 42 S. W. Hong, J. Xia, M. Byun, Q. Zou and Z. Q. Lin, *Macromolecules*, 2007, **40**, 2831.
- 43 S. W. Hong, J. Xia and Z. Q. Lin, *Adv. Mater.*, 2007, **19**, 1413.
- 44 S. W. Hong, M. Byun and Z. Q. Lin, *Angew. Chem., Int. Ed.*, 2009, **48**, 512.
- 45 J. Xu, J. Xia and Z. Q. Lin, *Angew. Chem., Int. Ed.*, 2007, **46**, 1860.
- 46 J. Wang, J. Xia, S. W. Hong, F. Qiu, Y. Yang and Z. Q. Lin, *Langmuir*, 2007, **23**, 7411.
- 47 M. Byun, S. W. Hong, F. Qiu, Q. Zou and Z. Lin, *Macromolecules*, 2008, **41**, 9312.
- 48 M. Byun, S. W. Hong, L. Zhu and Z. Q. Lin, *Langmuir*, 2008, **24**, 3525.